

Towards Understanding the Symmetry of Human Ears: A Biometric Perspective

Ayman Abaza and Arun Ross

Abstract—In this paper, an analysis of the symmetry of human ears is presented. Such an analysis is essential in order to understand the possibility of matching the left and right ears of an individual, or to reconstruct portions of the ear that may be occluded in a surveillance video. Ear symmetry is assessed geometrically using symmetry operators and Iannarelli’s measurements, where the contribution of individual ear regions to the overall symmetry of the ear is studied. Next, to assess the ear symmetry (or asymmetry) from a biometric recognition system perspective, several experiments were conducted on the WVU Ear Database. Our experiments suggest the existence of some degree of symmetry in the human ears that can perhaps be systematically exploited in the design of commercial ear recognition systems. At the same time, the degree of asymmetry it offers may be used in designing effective fusion schemes that combine the face information with the two ears.

I. INTRODUCTION

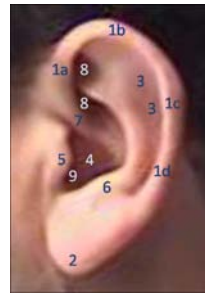
The appearance, structure and morphology of the human ear has been studied as a biometric cue for a number of years [1]. While most face recognition systems utilize the frontal attributes of the human face, the visibility of the ear in non-frontal poses of the face make it a viable biometric in many scenarios. The human ear is observed to exhibit variations across individuals as assessed by the curves and geometric measurements pertaining to the pinna or the auricle (the main part of the external ear). The anatomy of the pinna depicting the individual components can be seen in Figure 1.

A typical ear biometric recognition system consists of the following modules:

- 1) Preprocessing Stage:
 - a) Ear detection: Localizing the spatial extent of the ear in the given image.
 - b) Image normalization (Optional): Photometric (e.g., histogram equalization) and geometric (e.g., alignment) normalization of the localized ear prior to further processing.
 - c) Ear edge segmentation/localization (Optional): Finding the external contour of the ear and tracing the curves constituting the interior portion of the ear.
- 2) Feature Extraction Stage: Representing the structure of the ear using attributes such as geometrical measurements.

A. Abaza is with West Virginia High Technology Consortium Foundation, Fairmont, USA. aabaza@wvhtf.org. Abaza is also affiliated with Cairo University, Egypt.

A. Ross is with the Lane Department of Computer Science and Electrical Engineering, West Virginia University, Morgantown, USA. arun.ross@mail.wvu.edu



- (1) Helix Rim
- (2) Lobule
- (3) Antihelix
- (4) Concha
- (5) Tragus
- (6) Antitragus
- (7) Crus of Helix
- (8) Triangular Fossa
- (9) Incisure Intertragica

Fig. 1. External anatomy of the ear

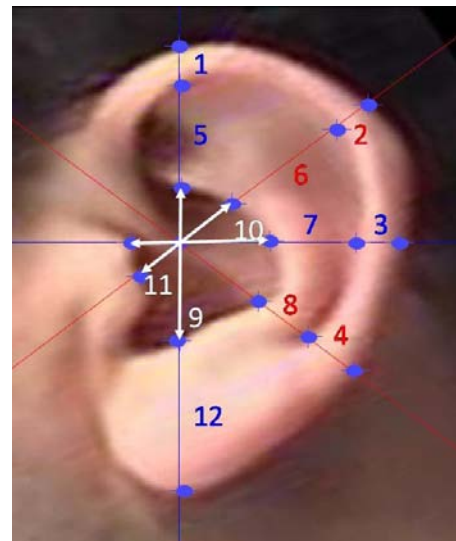


Fig. 2. Iannarelli measurement

- 3) Classification Stage (Optional): Classifying the ear into one of several sub-classes based on the ear shape. This is still an open research area in ear biometrics.
- 4) Matching Stage: Matching the probe feature set against the gallery feature set in the database. In verification mode, the subject claims an identity and the system verifies that claim by matching the probe only against the specified gallery. In identification mode, the system searches the entire gallery (database) in order to determine the identity of the person.

The use of the ear for human identification began with the development of the Iannarelli System [3]. This system is based upon 12 geometric measurements of the ear as illustrated in Figure 2. Here, the photograph of the ear is

placed on a development easel and geometrically aligned such that the lower tip of a standardized vertical guide on the development easel touches the upper flesh line of the cocha area whilst the upper tip touches the outline of the antitragus. The crus of helix is then detected and used as the origin. Vertical, horizontal, diagonal, and anti-diagonal lines are drawn from the origin to intersect with the internal and external edges present in the pinna resulting in 12 geometric measurements. These measurements have been used to distinguish individuals.

Currently, there are no commercial biometric systems that automatically verify identity based on the ear biometric alone. In the literature, Moreno and Sanchez [2] were the first to describe a fully automated ear recognition system. Their system relied on multiple features pertaining to the contour of the outer ear, and the shape and wrinkle information contained in the ear image to establish identity. Prior to that Burge and Burger [4] studied the possibility of automated ear recognition. Their method localized the ear in an image by using deformable contours on a Gaussian pyramid representation of the gradient image. Next, a sequence of edge extraction and curve extraction schemes were used to build a graph model of the ear. A graph matching scheme was used to assess the similarity of two ears. Chang et al. [5] developed an intensity-based ear recognition technique based on the Principal Component Analysis (PCA). Cadavid and Abdel-Mottaleb [6], developed a sophisticated technique for ear recognition from videos. They reconstructed the 3D shape of a ear (a 2.5D model) by using the Shape from Shading (SFS) technique. The Iterative Closest Point (ICP) algorithm was then used to calculate the similarity between the 3D shapes of two ear videos.

Human ears are located on both sides of the face and, therefore, the issue of symmetry of the structure of the two ears is a subject of interest. Such an analysis has several implications in a practical recognition system. One, if symmetry is established, then the left ear of an individual's probe image can be matched against their right ear in the gallery database (or vice-versa). Second, reconstructing partially occluded ear images will be possible, if information about the other ear is available. Third, if the ears of an individual are greatly asymmetrical, then this provides additional information about their identity.

II. EAR DEVELOPMENT AND ANATOMY

During the seventh week of pregnancy, the baby's face takes on more definition, as a mouth perforation, tiny nostrils and ear indentations become visible. The ear development during pregnancy is marked by the following highlights [7]:

- The auricle is developed from auricular hillocks that form in the 5th week.
- In the 7th week, the auricular hillocks begin to enlarge, differentiate and fuse, producing the final shape of the ear, which is gradually trans-located from the side of the neck to a more cranial and lateral site.
- The external ear forms from tissues of the first and second pharyngeal arches, as shown in Figure 3. This

figure is taken from [8]. Six tissue elevations, termed as auricular hillocks, become apparent. Three form from the first arch (Tragus, Helix, and Cymba concha) and the rest from the second arch (Antitragus, Antihelix, and Concha).

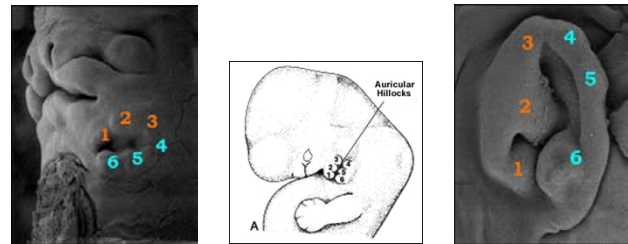


Fig. 3. Lateral views of human fetus at the sixth (Left) and ninth (Right) week, respectively. Taken from [8].

Thus, the ear does not have a completely random structure; it is made up of standard features just like the face is made up of some standard components. The shape of the ear tends to be dominated by the helix rim and the lobule shape. The anti-helix runs roughly parallel to the outer helix. The external anatomy of the ear [9] is illustrated in Figure 1.

III. FACE AND EAR SYMMETRY

Face symmetry has been used in biometrics to address the problem of pose variations [10]. Gutta et al. [11] investigated the use of half-of-the-face for matching by exploiting its symmetry and demonstrated that the recognition performance only reduced by 1%. The phenomena of face not being *perfectly* symmetrical has been well established in psychology. There is a narrow yet notable margin between perfect-symmetry and natural facial asymmetry. The effect of asymmetrical status on facial beauty was first investigated by Grammer and Thornhill [12] in 1994.

Liu et al. [13] were the first to investigate the effect of facial asymmetry on matching performance and their main objective was to enhance recognition performance under variations in expression. They demonstrated that face asymmetry provides useful information for human identification. Kompanets [14] investigated the bilateral asymmetry of the face in more detail. One interesting contribution of his research was the idea of a "truthful" vertical axis for the face and a special virtual coordinate system for the eye region. Another was the analysis of various facial components and their effect on face symmetry. However, to the best of our knowledge, the issue of *quantitatively* assessing the symmetry of the face is an ongoing research problem.

In the area of ear biometrics, Xiaoxun and Yunde [15] conducted an experiment similar to the the one presented by Zuo et al. [16] for face asymmetry. Images of the two ears of an individual were concatenated into a single image (as shown in Figure 5(a)) and used for feature extraction and classification. This concatenated image showed between 1 – 2% enhancement in performance compared to using the left or right ear alone. Yan and Bowyer [17] conducted a small experiment to test the ear symmetry using 119 subjects

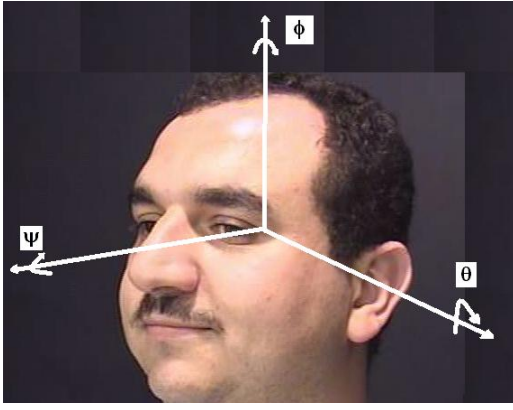


Fig. 4. Example from WVU database, where the rotation angles Φ the azimuth (raw), Θ the pitch, and Ψ the roll are presented.

under two poses. The right ear of the subject was used as the gallery and the left ear was used as the probe. By analyzing the results they concluded that most people's left and right ears are symmetric to a good extent, but that some people's left and right ears have different shapes.

In this work we perform detailed experiments to study ear symmetry from a biometric perspective. In this regard, we conduct three different analysis. In the first analysis, we use a symmetry operator to study the symmetry of the left and right ears. In the second analysis, we use the Iannerelli System to study the geometrical symmetry between individual regions in the left and right ears. In the third analysis, we use two ear recognition techniques to study the symmetrical properties of the ear.

Experiments are conducted using the West Virginia University data set (see appendix for more details). This data set was collected between 2006 and 2008. The raw data consists of a video sequence that images the human face at a rate of 3 frames per second in a 180° arc representing the rotation about \emptyset (as shown in Figure 4). This records the face and ear information of a subject over a duration of approximately 110 seconds. The pose angle of the face is calculated based on the frame number due to the deterministic nature of the acquisition procedure. However, these angles should still be considered as approximate values due to human and mechanical factors.

IV. EAR SYMMETRY OPERATOR

To assess the symmetry of the ears, we concatenated the left and right ears (as shown in Figure 5). We applied the symmetry transform suggested by Reisfeld et al. [18]. This discrete symmetry operator can estimate symmetricity by assigning a symmetry measure to each point in the edge map of the image. For a point p denoted as $p(x, y)$, the symmetry magnitude $S(p)$ is the accumulated contribution of those edge points $\Gamma(p)$ having p as middle point:

$$S(p) = \sum_{(i,j) \in \Gamma(p)} C(p_i, p_j) \quad (1)$$

where (p_i, p_j) are pair of points belonging to $\Gamma(p)$. The symmetry contribution $C(p_i, p_j)$ is defined based on the

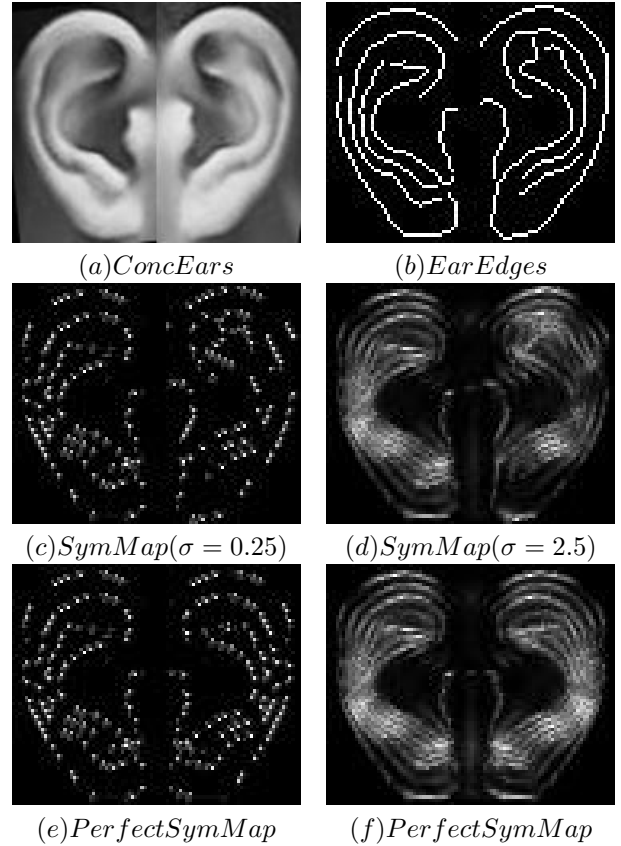


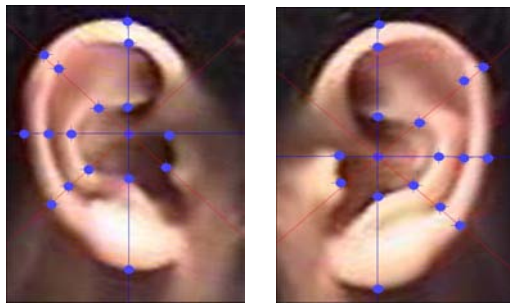
Fig. 5. Symmetry maps for concatenated left/right ear image compared to the concatenated right/flipped right ear images. (a) Original image and (b) its corresponding edge image. (c) and (d) Symmetry maps using small and large values for σ respectively; (e) and (f) The ideal symmetry map for the right ear and its mirror image

gradients (g_x, g_y) as follows:

$$\begin{aligned} C(p_i, p_j) &= D_\sigma(p_i, p_j) \cdot Ph(p_i, p_j) \cdot m_{p_i} \cdot m_{p_j} \quad (2) \\ m_p &= \log(1 + \sqrt{(g_x)^2 + (g_y)^2}) \\ D_\sigma(p_i, p_j) &= \frac{1}{\sqrt[2]{2\pi\sigma}} \cdot \exp\left(-\frac{\|p_i - p_j\|}{2\sigma}\right) \\ Ph(p_i, p_j) &= (1 - \cos(\theta_i + \theta_j - 2\alpha_{ij}))(1 - \cos(\theta_i - \theta_j)) \\ \theta &= \arctan(g_y/g_x) \\ \alpha_{ij} &= \arctan((y_j - y_i)/(x_j - x_i)) \end{aligned}$$

where σ controls the scope of the function. The aforementioned transform assigns a symmetry magnitude to every pixel in the image to construct a symmetry map. We constructed these symmetry maps for concatenated left and right ears using two different values for σ (0.25 and 2.5, respectively) as shown in Figure 5). We also constructed what we call the perfect symmetry map, by concatenating the right ear and its mirror image. We visually compared the two maps and observed that the symmetry maps of the concatenated left and right ears are very similar to the corresponding perfect symmetry map thereby suggesting the existence of symmetry for a majority of individuals.

Hayfron-Acquah et al. [19] used the Euclidean distance, to match the symmetry maps of gait sequences in the fourier domain. We followed this method to quantify the difference



Meas.	Right Ear		EER
	Left	Right	
1	25.33	26.67	37.56%
2	26.88	27.21	39.02%
3	18.00	18.00	41.62%
4	26.19	23.60	38.53%
5	52.33	46.00	39.67%
6	46.44	43.63	34.46%
7	34.33	30.33	37.80%
8	24.06	27.35	36.72%
9	75.00	82.00	35.42%
10	47.33	49.67	38.11%
11	43.40	49.98	40.15%
12	61.33	63.33	33.84%

Fig. 6. Iannarelli’s measurements for the left and right ears of a single subject. Also shown is the Equal Error Rate (EER) when using the corresponding measure alone for performing ear verification.

between the symmetry maps and perfect symmetry maps, shown in Figure 5). We constructed 309 symmetry maps for 309 subjects (using left and right ears) from the WVU database, and the perfect symmetry maps using only the left ears. We calculated the difference between these two sets of symmetry maps and performed the pairwise t-test to determine significance of these differences. The results indicated the existence of a certain degree of symmetry as assessed by these maps.

V. EAR GEOMETRICAL MEASUREMENTS

In a semi-automated mode, we extracted Iannarelli’s measurements for 618 images representing 309 different subjects (left and right ear images for each subject). Figure 6 shows samples of 2 subjects, where the Iannarelli’s measurements for the left and right ears are extracted and tabulated.

- Measurements 1-4 represent the helix rim, or outer ear curves.
- Measurement 5 represents part of the triangular fossa, and 6-8 the antihelix, or the distance from the internal curves to the external curves.
- Measurements 9-11 represent part of the triangular fossa, and the concha, or the internal curves of the ear.
- Measurement 12 represents the lobule length.

Statistically, we performed the paired t-test for the difference of each corresponding measurement pair (example of corresponding measures is shown in Figure 6). We repeated this paired t-test 12 times; all the measurements, except 4

and 11, indicate certain degree of symmetry between the left and right ears.

A verification experiment using these 309 subjects was setup. For each subject, the left ear was used as the gallery while the right ear was used as the probe. The Euclidian distance was used for matching. The Equal Error Rate (EER) for such an experiment was 16.75%. When analyzing the performance of each of the Iannarelli’s measurement separately, we observe that measurements 3 and 11 resulted in the least performance. While some of these errors may be attributed to human errors (since the magnitude of measurement 3 is rather small), the profile angle of the ear can also affect the horizontal and diagonal measurements. Another reason is that some people’s left and right ears have different shapes by nature (as shown in Figure 7) or due to disease / usage of accessories.

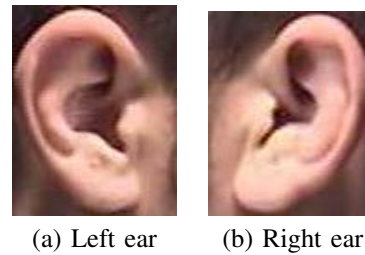


Fig. 7. A subject with markedly different left and right ears.

VI. SYMMETRY ASSESSMENT USING EAR MATCHERS

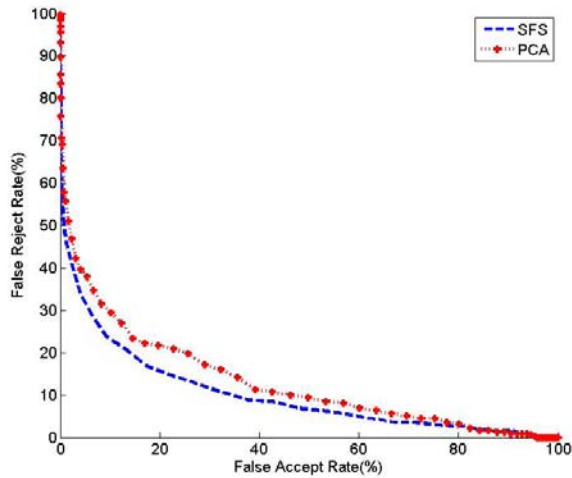
Two ear matchers alluded to earlier were used in this experiment: the Shape From Shading (SFS) [6] and Eigen-Ear (PCA) [5] technique. For ear detection from profile face images in the WVU Ear Database, we used the morphological segmentation technique proposed by Hajsaid et al. [20]. We excluded cases in which the automated segmentation techniques resulted in errors; thus, we considered 320 subjects in this analysis, and 38 of these subjects had multiple video sequences.

To test the existence of symmetry, we set up a verification experiment using 320 left ear images (at angles ~ 20) as the gallery and 320 reflected right ear images (at angles ~ 160) as the probe. These angles are approximately calculated based on the frame number. The results are shown in Figure 8-a:

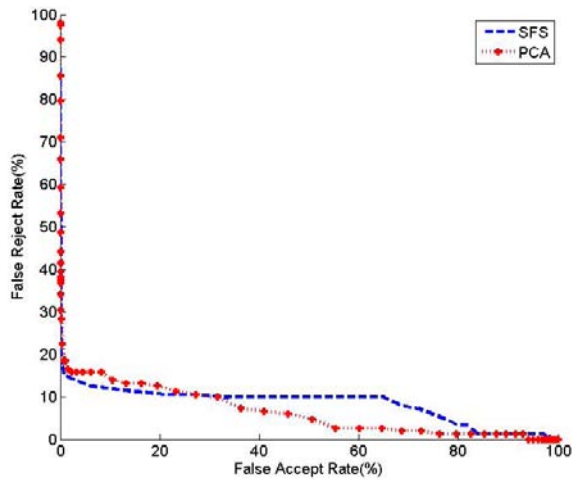
- For the SFS technique, the EER = 17.06%.
- For the PCA technique, the EER = 21.05%.

In order to interpret the numbers above, we need to first establish the baseline performance of the two matchers used in this work. To assess this baseline performance, 152 right ear probes (4 images taken from each of the repeated sequences at angles $\sim 157.5, \sim 160, \sim 162.5, \text{ and } \sim 165$) were compared against 320 right ear images (gallery images at approximately the same angles). The results are as follows (shown in Figure 8):

- For the SFS technique, the EER = 11.12%.
- For the PCA technique, the EER = 13.21%.



(a)

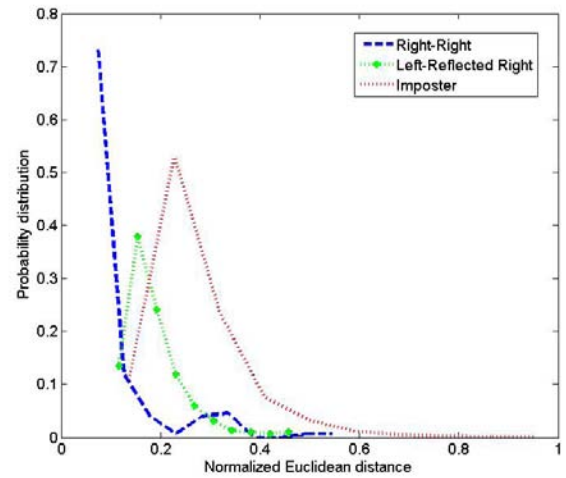


(b)

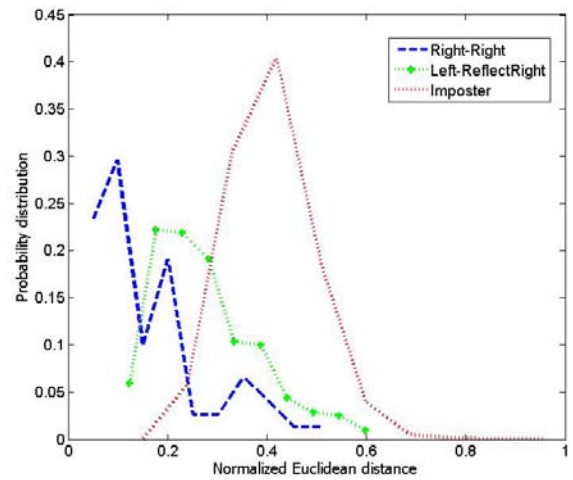
Fig. 8. Ear verification results using a) the left ear image as gallery and the reflected right ear as probe; b) using probe and gallery from different video sequences

By comparing the results of these two experiments, we can estimate that the effect of ear asymmetry affects the recognition rate by a magnitude between 5.94% and 7.84%. For further analysis, Figure 9 shows the probability distribution of the match scores from these two experiments. This figure shows the score distribution of matching images of the same ear (right vs right); matching the left ear with the reflected right ear for the same subject (left vs reflected right); and the impostor matchings of the left ear. The question is whether the difference in scores between “right vs right” and “left vs reflected right” (d_1) is significantly different from the difference in scores between “right vs right” and “impostor” (d_2). The t-test shows $|d_1 - d_2|$ to be significantly different with p-value < 0.01 .

To quantify the effect of ear asymmetry on the recognition performance, we repeated the previous experiments in the



(a) SFS



(b) PCA

Fig. 9. Match score distribution of the genuine scores of “right vs right” and “left vs reflected right” ears, compared to impostor scores.

identification mode. The results are as follows (shown in Figure 10):

- Using the reflected probe set:
 - For the SFS technique, rank1 = 49.06% and rank 10 = 71.56%.
 - For the PCA technique, rank1 = 35.31% and rank 10 = 63.44%.
- Using the original probe and gallery (i.e., no reflection):
 - For the SFS technique, rank1 = 84.87% and rank 10 = 88.16%.
 - For the PCA technique, rank1 = 73.68% and rank 10 = 84.87%.

These results suggest that the asymmetry of the two ears *does affect* the identification performance, where the rank-1 accuracy is observed to drop by an absolute value of $\sim 35\%$.

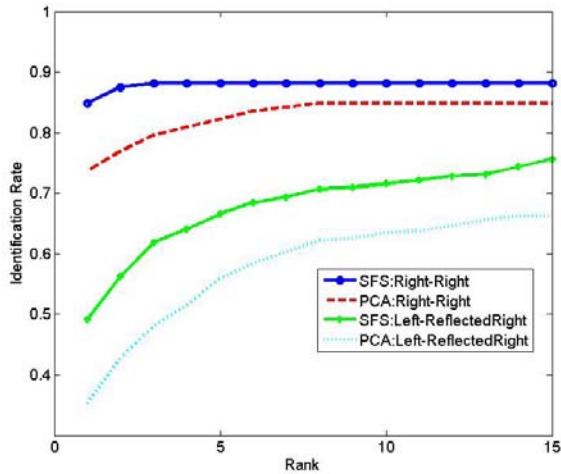


Fig. 10. Ear identification results using the left ear image as gallery and the reflected right ear as probes

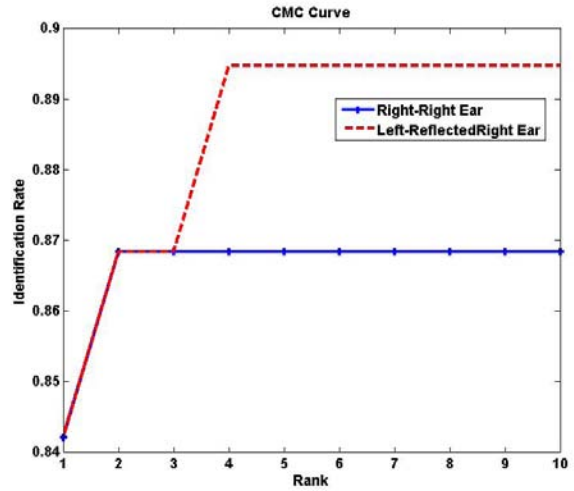


Fig. 11. Ear identification results of fusing the scores of “right vs right” and “left vs reflected right”.

VII. CASE STUDY

As an application for ear (a)symmetry, we assumed a scenario in which both ear images of a subject (i.e., left and right) are available in the database, while only one of the ears is acquired as a probe. We set up two experiments as follows:

- We used the SFS technique to perform matching.
- We generated scores using probes and gallery images of the same sided ear, i.e., right vs right.
- We generated scores using the left ear image as a gallery image and the reflected right ear as the probe image.
- We fused the scores of these two sets using the weighted sum rule. We defined the weights based on rank one performance of each set.

This fusion enhances the rank-4 performance by an absolute value of $\sim 3\%$ as shown in Figure 11.

VIII. CONCLUSION AND FUTURE WORK

In this paper, we attempted to analyze the symmetry of the two ears. First, ear symmetry was tested using a geometrical symmetry operator. Next, Iannarelli’s measurements were used to assess the degree of symmetry of individual ear regions. Finally, various recognition experiments were conducted to test for ear symmetry. Overall, the experimental results in the verification mode indicate that left and right ears are symmetric only to *some extent*. Thus, there is a degree of asymmetry as well. To assess the degree of asymmetry, we repeated the same experiments in the identification mode. These identification experiments indicate that when matching a left ear image with a reflected right ear image of the same individual, the rank-1 performance drops by 35%; however, retrieving more images may be beneficial in identifying a match.

Future plans include designing parametric models for the ear edges and using them to quantify the symmetry of individual ear parts. Another extension is to use the ear

(a)symmetry to help solve other problems as occlusion due to hair and variations in ear poses.

IX. APPENDIX: WVU EAR DATABASE

The West Virginia University (WVU) ear database was collected using the system shown in Figure 12[21]. This system has undergone various design, assembly, and implementation changes since then. The main hardware components for this system include the following:

- PC: Provides complete control over the moving parts and acquires video from the camera.
- Camera: Captures video. It is attached to the camera arm which is controlled by a stepper motor.
- Linear Actuator: This is a unique custom-made device (by Netmotion, Inc.) that has a 4-ft span and allows for smooth, vertical (up or downward) translation. This device is used to adjust the height of the camera according to the subject’s sitting height.
- Light: For assembling this database, the light was fixed to the camera arm. In other words, the light arm shown in Figure 12 was not used.
- Structural Framework: Consisted of tinted wall, rotating arms, and other structural supports. A black board was added behind the chair, to serve as a uniform background during video capture.

There are various software packages that were used:

- Posteus IPE (stepper system control): to adjust the camera height, and to rotate the camera.
- EVI Series Demonstration Software (camera control): to adjust zoom, tilt, and focus of the camera.
- IC Video Capture: to record the different poses of the subject’s face during camera rotation.

The WVU ear database consists of 460 video sequences of 402 different subjects, and has multiple video sequences for 54 subjects [22]. Each video begins at the left profile

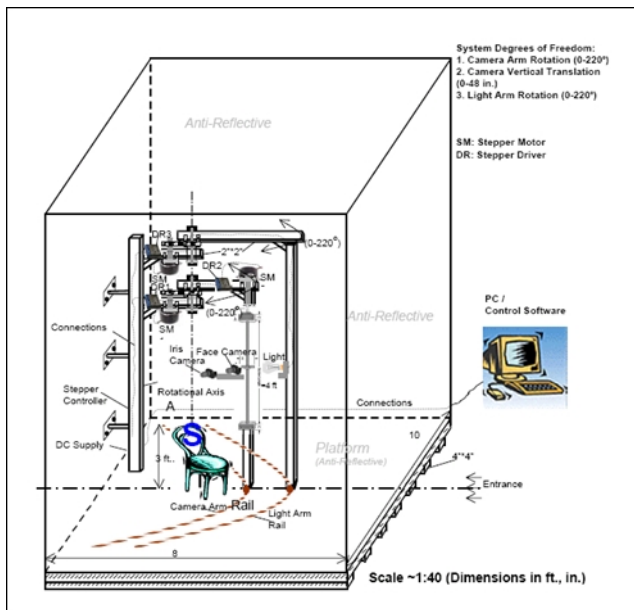


Fig. 12. Schematic diagram of the data acquisition system

(0 deg) of the subject, and takes about 2 minutes to end at the right profile (180 deg). This database has 55 subjects with eyeglasses, 42 subjects with earrings, 38 subjects with partially occluded ears, and 2 subjects with fully occluded ears.

X. ACKNOWLEDGMENTS

The data collection process was funded by the FBI Academy. Ross was supported by FBI Grant Number A9A906229. Abaza started this project when he was in West Virginia University and resumed it in WVHTF where he was supported by ONR under Contract No. N00014-09-C-0388. The authors are grateful to Dr. Mohammed Abdel-Mottaleb and Steven Cadavid (University of Miami) for sharing their ear recognition code. The authors would like to thank Dr. Ahmed Fikry Attaallah (West Virginia University Hospitals) for discussions about ear growth.

REFERENCES

- [1] D. Hurley, B. Arbab-Zavar, and M. Nixon, "The Ear as a Biometric," in A. Jain, P. Flynn and A. Ross, "Handbook of Biometrics", chapter 7, Springer US, 2007, pp. 131-150.
- [2] B. Moreno, and A. Sanchez, "On the Use of Outer Ear Images for Personal Identification in Security Applications," in the 33rd International Conference on Security Technology, 1999, pp. 469-476.
- [3] A. Iannarelli, *Ear Identification, Forensic Identification Series*, Paramount Publishing Company, Fremont, California, 1989.

- [4] M. Burge, and W. Burger, "Ear Biometrics in Computer Vision," *15th International Conference of Pattern Recognition (ICPR)*, 2000, pp. 826-830.
- [5] K. Chang, K. Bowyer, S. Sarkar, and B. Victor, "Comparison and Combination of Ear and Face Images in Appearance-Based Biometrics," *IEEE Transactions on Pattern Analysis and Machine Intelligence (PAMI)*, vol. 25, no. 9, Sept. 2003, pp. 1160-1165.
- [6] S. Cadavid, and M. Abdel-Mottaleb, "3D Ear Modeling and Recognition from Video Sequences using Shape from Shading," *IEEE Transactions on Information Forensics and Security*, vol. 3, no. 4, Dec 2008, pp. 709-718.
- [7] David Boshell, Ear Development
http://download.videohelp.com/vitalis/med/Ear_Devt.html.
- [8] Units of Embryo Images
http://www.med.unc.edu/embryo_images/unit-ear/ear_hmtm/ear014.htm.
- [9] M. Bermant, Bermant Plastic Surgery
http://www.plasticsurgery4u.com/procedure_folder/otoplasty_anatomy.html.
- [10] S. Malassiotis, and M. G. Strintzis, "Robust face recognition using 2D and 3D data: Pose and illumination compensation," *Pattern Recognition*, vol. 38, no. 12, Dec 2005, pp. 2537-2548.
- [11] S. Gutta, V. Philomin, and Miroslav Trajkovic, "An Investigation into the Use of Partial-Faces for Face Recognition," in the *Fifth IEEE International Conference on Automatic Face and Gesture Recognition (FGR)*, Washington DC, 2002, pp. 33-38.
- [12] K. Grammer, and R. Thornhill, "Human (Homo sapiens) facial attractiveness and sexual selection: The role of symmetry and averageness," *Journal of Comparative Psychology*, vol.108, no.3, 1994, pp. 233-242.
- [13] Y. Liu, R. L. Weaver, K. Schmidt, N. Serban, and J. Cohn, "Facial Asymmetry: A New Biometric," *technical report CMU-RI-TR-01-23*, Robotics Institute, Carnegie Mellon University, Aug 2001, pp. 1-21.
- [14] L. Kompanets, "Biometrics of asymmetrical face," *First International Conference on Biometric Authentication (ICBA)*, 2004, pp. 67-73.
- [15] Z. Xiaoxun, and J. Yunde, "Symmetrical Null Space LDA for Face and Ear Recognition," *Neuro-computing*, vol. 70, no.4-6, 2007, pp. 842-848.
- [16] W. Zuo, K. Wang, and D. Zhang, "Improvement on Null Space LDA for Face Recognition: A Symmetry Consideration," *Second International Conference on Biometric Authentication (ICBA)*, 2006, pp. 78-84.
- [17] P. Yan, and K. Bowyer, "Empirical Evaluation of Advanced Ear Biometrics," in the *IEEE Computer Vision and Pattern Recognition (CVPR)*, vol. 3, Washington - DC, Jun 2005, pp. 41-48.
- [18] D. Reisfeld, H. Wolfson, and Y. Yeshurun, "Context-free attentional operators: The generalized symmetry transform," *International Journal of Computer Vision*, vol. 14, no. 2, 1995, pp. 119-130.
- [19] James Hayfron-Acquah, Mark Nixon, and John Carter, "Automatic gait recognition by symmetry analysis," *Pattern Recognition Letter*, vol. 24, no. 13, Sep. 2003, pp. 272-277.
- [20] E. HajSaid, A. Abaza, and H. Ammar, "Ear Segmentation in Color Facial Images Using Mathematical Morphology", *6th Biometric Consortium Conference*, Tampa-FL, 2008, pp. 29-34.
- [21] G. Fahmy, A. Elsherbeeney, S. Mandala, M. Abdel-Mottaleb, and H. Ammar, "The effect of lighting direction/condition on the performance of face recognition algorithms," *SPIE Conference on Biometrics for Human Identification*, vol. 6202, Apr 2006, pp. 188-200.
- [22] Ayman Abaza, "High Performance Image Processing Techniques in Automated Identification Systems," PhD Dissertation, Lane Department of Computer Science and Electrical Engineering, West Virginia University, USA, 2008.